Sains Malaysiana 51(8)(2022): 2669-2680
http://doi.org/10.17576/jsm-2022-5108-25

Radiative Non-Coaxial Rotating Flow for Viscous Fluid over Accelerated Disk with MHD and Porosity Effects

(Aliran Beradiasi yang Berputar Tidak Sepaksi bagi Bendalir Likat Melepasi Cakera Bergerak dengan Kesan Magnetohidrodinamik dan Keliangan)

WAN NURA'IN NABILAH NORANUAR[1], AHMAD QUSHAIRI MOHAMAD[1,*], LIM YEOU JIANN[1], SHARIDAN SHAFIE[1] & DENNIS LING CHUANG CHING[2]

[1]*Department of Mathematical Sciences, Faculty of Science, Universiti Teknologi Malaysia, 81310 Johor Bahru, Johor Darul Takzim, Malaysia*
[2]*Department of Fundamental and Applied Sciences, Universiti Teknologi PETRONAS, Seri Iskandar, 32610 Tronoh, Perak Darul Ridzuan, Malaysia*

Received: 25 October 2021/Accepted: 25 January 2022

ABSTRACT

An analytical solution to analyze the effects of radiation, magnetic, and permeability in an accelerating non-coaxial rotation phenomenon is not yet reported in the previous studies. Therefore, a radiative mixed convection flow for non-coaxial rotating MHD viscous fluid in a porous medium past an accelerated disk is studied. The fluid motion in this problem is induced by two sources which are rotating and buoyancy force. The dimensional coupled differential equations subjected to initial and accelerated boundary conditions are transformed to the dimensionless equations by utilizing appropriate dimensionless variables. The Laplace transform technique is applied to generate the closed form analytical solution for this problem. The impacts of Prandtl number, Grashof number, radiation, magnetic, porosity, and accelerated parameters on the temperature and velocity fields are illustrated graphically. The velocity and temperature profiles satisfy both the initial and boundary conditions, and the present results are found in accordance to the published work. The velocity is improved with the assistance of acceleration, radiation and porosity, while the implementation of magnetic field causes the opposite effect. Increasing radiation leads to the growth of the thermal boundary layer as well as reducing the heat transmission rate. This result can significantly contribute to the designing of heating systems because the imposition of radiation able to sustain an environment for a specific temperature. The obtained analytical solution can be used to check the correctness of the solution obtained from the numerical and experimental studies.

Keywords: Accelerated disk; heat transfer; Laplace transform; non-coaxial rotation; radiation

ABSTRAK

Penyelesaian analitik untuk menganalisis kesan radiasi, magnetik dan keliangan dalam fenomena putaran tidak sepaksi yang terpecut belum pernah dilaporkan dalam kajian terdahulu. Oleh itu, aliran olakan campuran beradiasi bagi bendalir likat magnetohidrodinamik yang berputar tidak sepaksi di dalam bahantara berliang melepasi cakera terpecutkan dikaji. Pergerakan bendalir untuk masalah ini adalah disebabkan oleh dua sumber iaitu kesan daya putaran dan daya apungan. Persamaan pembezaan gandingan bermatra tertakluk kepada syarat awal dan syarat sempadan terpecutkan dijelmakan kepada persamaan tak bermatra dengan menggunakan pemboleh ubah tanpa matra yang sesuai. Teknik penjelmaan Laplace digunakan untuk menghasilkan penyelesaian analitik tertutup bagi masalah ini. Kesan nombor Prandtl, nombor Grashof, radiasi, magnet, keliangan dan parameter terpecutkan terhadap profil suhu dan halaju diilustrasikan dalam bentuk graf. Profil halaju dan suhu memenuhi kedua-dua syarat awal dan syarat sempadan dan keputusan kajian ini didapati selari dengan hasil kajian terdahulu. Halaju dipertingkatkan dengan bantuan pecutan, radiasi dan keliangan, manakala kehadiran medan magnet menyebabkan kesan sebaliknya. Peningkatan radiasi membawa kepada pertumbuhan lapisan sempadan haba serta mengurangkan kadar pemindahan haba. Keputusan ini boleh menyumbang dengan ketara dalam mereka bentuk sistem pemanasan kerana pengenalan sinaran mampu mengekalkan persekitaran untuk suhu tertentu. Penyelesaian analitik yang diperoleh boleh digunakan untuk menyemak ketepatan penyelesaian yang diperoleh daripada kajian berangka dan uji kaji.

Kata kunci: Cakera terpecutkan; pemindahan haba, penjelmaan Laplace; putaran tak sepaksi; radiasi

Introduction

The flow of a non-coaxial rotating viscous fluid has gained much attention and have been explored by many researchers. Becker (1963) generated an exact solution to investigate this type of flow within two identical angular velocity disks. The exact solution obtained in solving the problem is important as this could be a verification and benchmark for the solution obtained by a numerical and approximate method. This study is resumed by Erdogan (2000), where the time-dependent Navier-Stokes equation in the non-coaxial rotation flow for the case of an oscillating disk was considered. Guria et al. (2007) developed a model for a non-coaxial rotating viscous fluid that flows unsteadily within magnetic field. Hayat et al. (2008) continued the previous study by considering a flow that is bounded by an oscillating disk and Asghar et al. (2007) considered a flow that is bounded by an accelerated disk. The flow subjected to this type of rotation was also done by Guria et al. (2009) and they considered a porous disk to investigate the unsteady viscous fluid flow under impacts of slip condition and hall current. Das and Jana (2014) studied the infinite flow of an MHD viscous fluid subjected to the same type of disk rotation. A similar problem was done by Guria (2018) where the rotating flow is affected by a periodic suction and the disks are rotating with a uniform angular velocity. Based on the mentioned studies, the problems were solved to obtain an exact solution for the velocity profile by adapting the Laplace transform method. These studies presented the solutions for momentum equation in a complex velocity form.

Thereafter, the work on non-coaxial rotation flow was explored with the incorporation of heat transfer analysis. Das et al. (2012) investigated the temperature profile and the rate of heat transmission. An analytical study for the heat transport in mixed convection flow was performed by Amin et al. (2020). Mohamad et al. (2016) considered a non-coaxially oscillating disk in investigating the heat transportation and flow regimes for a Newtonian fluid. Ersoy (2017) performed a similar study by considering a disk that is induced by non-torsional oscillations. Maji et al. (2010) studied the flow of non-coaxial rotation with porosity consequence where the fluid and disk have been placed in a porous medium. Magnetohydrodynamics (MHD) effect is created when the fluid that carries current is moved through the magnetic field, causing an augment of the Lorentz force. Bakar et al. (2019) considered MHD effect in analysing the heat transmission and fluid flow in a square cavity. They showed that the existence of magnetic field causes the fluid flow to be retarded. Mohamad et al. (2017) discussed this effect for a second grade fluid flow under a non-coaxial rotation in the presence of a porosity effect. Srivastava (2017) studied the flow features of an MHD fluid where the coaxial rotation of disks was considered at different speeds. Mohamad et al. (2018) analyzed the heat transfer and rotating flow behavior under impacts of porosity and MHD. The combined heat and mass transfer (double convection) model were also taken into account. Rafiq et al. (2018) expressed the closed form solution of a velocity profile for a Casson fluid with a non-coaxial rotation. Mahanthesh et al. (2019) continued the study by considering a similar Casson fluid where the flow is triggered by an oscillating non-coaxial rotation disk. Mohamad et al. (2020) conducted a study on a non-coaxial rotating flow due to an accelerated disk with MHD and porosity effects. The research was then expanded by Noranuar et al. (2021) by taking the effects of double convection into account.

Based on the above literature, the study of non-coaxial rotation flow generated by an accelerated disk under the effect of thermal radiation has not been investigated or found in any of the aforementioned studies. The most similar radiative non-coaxial rotation study was presented by Rana et al. (2020), but a stationary disk was considered. Incorporating with MHD and porosity effects, Noranuar et al. (2020) carried out a radiative heat and mass transmission analysis subjected to the same rotation for a moving disk. Ishak (2011) imposed the effects of radiation and MHD in investigating the boundary layer flow for a viscous fluid. Other references regarding the radiation impact on the unsteady flow of an MHD viscous fluid are available in Hussain et al. (2018), Pandit et al. (2018), Seth et al. (2014), and Zainuddin et al. (2016). Therefore, inspiring from the above study, this work is extended to investigate the impacts of radiation together with MHD and porosity on the time-dependent flow of a mixed convective viscous fluid caused by a non-coaxial rotation and passes through an accelerated disk. The closed form solutions for the temperature and velocity profiles in the form of complementary and exponential functions are attained by employing the Laplace transform method. The results are presented graphically and numerically with a comprehensive discussion.

Problem Formulation

Consider a mixed convective flow of an unsteady incompressible electrically conducting viscous fluid with MHD effect in a non-coaxial rotation. Both fluid and disk

are saturated in a porous medium as depicted in Figure 1. A rigid disk at $z = 0$ is used to bound the fluid flow. The fluid occupies the space $z > 0$ and is moving in the z direction which is defined to be normal to the disk while the upward direction along the disk is denoted by x-axis. The plane $x = 0$ is considered to be the axes for the fluid and disk to rotate. A magnetic field of uniform strength, B_0, is imposed transversely to the disk. The disk and fluid at infinity are rotating about z'-axis when time $t = 0$ with an angular velocity Ω at temperature T_∞. After time $t > 0$, the disk starts to accelerate and rotate with the same angular velocity Ω about z-axis while the fluid at infinity remains to rotate about the z'-axis as that of the disk with the same angular velocity Ω. The rotation axes have been separated by a distance ℓ and the disk temperature raises to T_w. Utilizing these assumptions and by considering the existence of a radiation effect, the concerned governing momentum and energy equations can be expressed as

$$\frac{\partial F}{\partial t} + dF = \nu \frac{\partial^2 F}{\partial z^2} + d\Omega\ell + g_x\beta_T(T - T_\infty), \tag{1}$$

$$\rho C_p \frac{\partial T}{\partial t} = k\frac{\partial^2 T}{\partial z^2} - \frac{\partial q_r}{\partial z} \tag{2}$$

with associated initial and boundary conditions

$$\begin{aligned} F(z,0) &= \Omega\ell; \quad T(z,0) = T_\infty; \quad z > 0, \\ F(0,t) &= A_1 t; \quad T(0,t) = T_w; \quad t > 0, \\ F(\infty,t) &= \Omega\ell; \quad T(\infty,t) = T_\infty; \quad t > 0, \end{aligned} \tag{3}$$

where $d = \Omega i + {}^{\nu}/_{k_1} + {}^{\sigma{\beta_0}^2}/_{\rho}$. In this study, the form of complex function is used to present the velocity solution $F = f + ig$, where f is the primary velocity (real part) and g is the secondary velocity (imaginary part) while T is the temperature function. Then, σ, ρ, ν, k_1, g_x, β_T, C_p, k, q_r and A_1 denoted for electrical conductivity, density of rotating fluid, kinematic viscosity, permeability of the porous medium, gravity, thermal expansion coefficient, specific heat capacity, thermal conductivity, radiative heat flux in z-direction and acceleration of the disk and fluid.

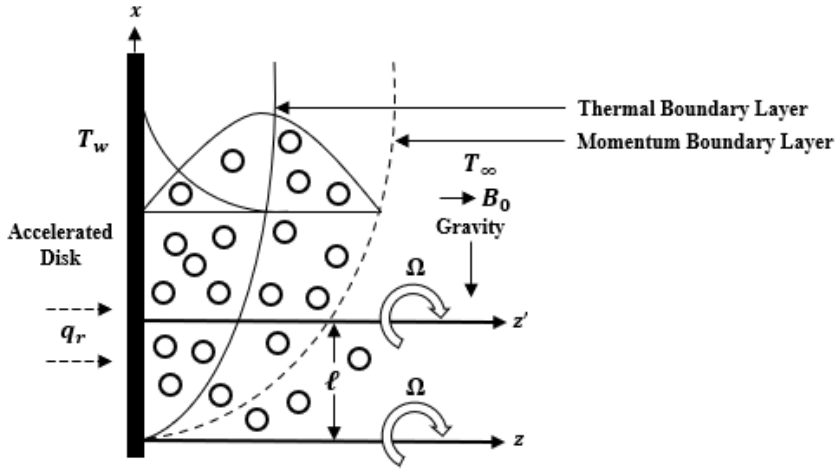

FIGURE 1. Geometry of the problem

Adopting the Rosseland approximation (Hussain et al. 2018; Pandit et al. 2018; Seth et al. 2014), the radiative heat flux takes the form as follows

$$q_r = -\frac{4\sigma^*}{3k^*}\frac{\partial T^4}{\partial z}, \tag{4}$$

in which k^* is the mean absorption coefficient and σ^* is the Stefan-Boltzmann constant. Next, assuming T^4 in (4) as a linear combination of temperature difference within the flow that has been expanded by Taylor series about T_∞ and omitting the higher order terms, it forms

$$T^4 \cong 4{T_\infty}^3 T - 3{T_\infty}^4. \tag{5}$$

In the view of substituting (4) and (5) into (2), the governing energy equation is simplified to

$$\rho C_p \frac{\partial T}{\partial t} = \left(k + \frac{16\sigma^* {T_\infty}^3}{3k^*}\right)\frac{\partial^2 T}{\partial z^2}. \tag{6}$$

Both governing equations, (1) and (6) with the conditions (3) are written in dimensionless form by substituting the following dimensionless variables as

$$F^* = \frac{F}{\Omega \ell} - 1, \quad z^* = \sqrt{\frac{\Omega}{\upsilon}} z, \quad t^* = \Omega t, \quad T^* = \frac{T - T_\infty}{T_w - T_\infty}. \tag{7}$$

The dimensionless form of the resulting equations is expressed as

$$\frac{\partial F}{\partial t} + d_1 F = \frac{\partial^2 F}{\partial z^2} + GrT, \tag{8}$$

$$\frac{\partial T}{\partial t} = \frac{1}{\mathrm{Pr}_1} \frac{\partial^2 T}{\partial z^2}, \tag{9}$$

corresponding to dimensionless conditions

$$\begin{gathered} F(z,0) = 0; \quad T(z,0) = 0; \quad z > 0, \\ F(0,t) = At - 1; \quad T(0,t) = 1; \quad t > 0, \\ F(\infty,t) = 0; \quad T(\infty,t) = 0; \quad t > 0, \end{gathered} \tag{10}$$

where

$$d_1 = i + \frac{1}{K} + M^2, \quad \mathrm{Pr}_1 = \frac{\mathrm{Pr}}{1 + Rd}, \quad \frac{1}{K} = \frac{\nu}{\Omega k_1}, \quad M = \frac{\sigma {\beta_0}^2}{\Omega \rho}, \quad \mathrm{Pr} = \frac{\mu C_p}{k},$$

$$Rd = \frac{16 \sigma^* {T_\infty}^3}{3k^*}, \quad Gr = \frac{g_x \beta_T (T_w - T_\infty)}{\Omega^2 \ell}, \quad A = \frac{A_1}{\Omega \ell}.$$

Here, d_1 and Pr_1 are constant parameters, while K, M, Pr, Rd, Gr and A represent porosity parameter, magnetic parameter (magnetic field), Prandtl number, radiation parameter, Grashof number and acceleration parameter.

EXACT EQUATION

After that, applying the technique of Laplace transform on the governing equations in (8-10), yields to the following expression

$$\frac{d^2 \bar{F}}{dz^2} - (q + d_1)\bar{F} = -Gr \frac{1}{q} exp\left(-z\sqrt{\mathrm{Pr}_1 q}\right), \tag{11}$$

$$\bar{F}(0,q) = \frac{A}{q^2} - \frac{1}{q}, \quad \bar{F}(\infty,q) = 0, \tag{12}$$

$$\frac{d^2 \bar{F}}{dz^2} - \mathrm{Pr}_1 q \bar{T} = 0, \tag{13}$$

$$\bar{T}(0,q) = \frac{1}{q}, \quad \bar{T}(\infty,q) = 0. \tag{14}$$

Next, the conditions in (12) and (14) are used to solve (11) and (13) which then become

$$\begin{aligned} \bar{F}(z,q) = \bar{F}_1(z,q) - \overline{F_2}(z,q) - \overline{F_3}(z,q) + \bar{F}_4(z,q) + \\ \overline{F_5}(z,q) - \overline{F_6}(z,q), \end{aligned} \tag{15}$$

$$\bar{T}(z,q) = \frac{1}{q} exp\left(-z\sqrt{\mathrm{Pr}_1 q}\right), \tag{16}$$

where

$$\bar{F}_1(z,q) = \frac{A}{q^2} exp\left(-z\sqrt{q + d_1}\right), \quad \overline{F_2}(z,q) = \frac{1}{q} exp\left(-z\sqrt{q + d_1}\right),$$

$$\overline{F_3}(z,q) = \frac{Gr_1}{q} exp\left(-z\sqrt{q + d_1}\right), \quad \bar{F}_4(z,q) = \frac{Gr_1}{q - d_3} exp\left(-z\sqrt{q + d_1}\right),$$

$$\overline{F_5}(z,q) = \frac{Gr_1}{q} exp\left(-z\sqrt{\mathrm{Pr}_1 q}\right), \quad \overline{F_6}(z,q) = \frac{Gr_1}{q - d_3} exp\left(-z\sqrt{\mathrm{Pr}_1 q}\right).$$

Then, employing the inverse Laplace transform on (15) and (16), the following exact velocity and temperature solutions are attained as

$$\begin{aligned} F(z,t) = F_1(z,t) - F_2(z,t) - F_3(z,t) + F_4(z,t) \\ + F_5(z,t) - F_6(z,t), \end{aligned} \tag{17}$$

$$T(z,t) = erfc\left(\frac{z}{2}\sqrt{\frac{\mathrm{Pr}_1}{t}}\right), \tag{18}$$

where

$$F_1(z,t) = \frac{A}{2} \int_0^t exp\left(-z\sqrt{d_1}\right) erfc\left(\frac{z}{2\sqrt{s}} - \sqrt{d_1 s}\right) + exp\left(z\sqrt{d_1}\right) erfc\left(\frac{z}{2\sqrt{s}} + \sqrt{d_1 s}\right) ds,$$

$$F_2(z,t) = \frac{1}{2}\left(exp\left(z\sqrt{d_1}\right) erfc\left(\frac{z}{2\sqrt{t}} + \sqrt{d_1 t}\right) + exp\left(-z\sqrt{d_1}\right) erfc\left(\frac{z}{2\sqrt{t}} - \sqrt{d_1 t}\right)\right),$$

$$F_3(z,t) = \frac{Gr_1}{2}\left(exp\left(z\sqrt{d_1}\right) erfc\left(\frac{z}{2\sqrt{t}} + \sqrt{d_1 t}\right) + exp\left(-z\sqrt{d_1}\right) erfc\left(\frac{z}{2\sqrt{t}} - \sqrt{d_1 t}\right)\right),$$

$$\begin{aligned} F_4(z,t) = \frac{Gr_1}{2}\Bigg(exp\left(d_3 t + z\sqrt{d_1 + d_3}\right) erfc\left(\frac{z}{2\sqrt{t}} + \sqrt{(d_1 + d_3)t}\right) \\ + exp\left(d_3 t - z\sqrt{d_1 + d_3}\right) erfc\left(\frac{z}{2\sqrt{t}} - \sqrt{(d_1 + d_3)t}\right)\Bigg), \end{aligned}$$

$$F_5(z,t) = Gr_1 exp\left(\frac{z}{2}\sqrt{\frac{\mathrm{Pr}_1}{t}}\right),$$

$$\begin{aligned} F_6(z,t) = \frac{Gr_1}{2}\Bigg(exp\left(d_3 t + z\sqrt{\mathrm{Pr}_1 d_3}\right) erfc\left(\frac{z}{2}\sqrt{\frac{\mathrm{Pr}_1}{t}} + \sqrt{d_3 t}\right) \\ + exp\left(d_3 t - z\sqrt{\mathrm{Pr}_1 d_3}\right) erfc\left(\frac{z}{2}\sqrt{\frac{\mathrm{Pr}_1}{t}} - \sqrt{d_3 t}\right)\Bigg), \end{aligned}$$

with $d_2 = \mathrm{Pr}_1 - 1, d_3 = {d_1}/{d_2}, Gr_1 = {Gr}/{d_2 d_3}$ are constant parameters.

PHYSICAL QUANTITIES

The skin friction τ for the plate is expressed as

$$\tau = -\left[\mu \frac{\partial F}{\partial z}\right]_{z=0}, \tag{19}$$

which after dimensionless process reduces to

$$\tau = -\left[\frac{\partial F^*}{\partial z^*}\right]_{z^*=0}. \tag{20}$$

In view of (17), it gives

$$\tau(t) = \tau_1(t) - \tau_2(t) - \tau_3(t) + \tau_4(t) + \tau_5(t) - \tau_6(t), \tag{21}$$

where

$$\tau_1(t) = \left(\frac{A}{2}\right)\int_0^t \frac{2}{\sqrt{\pi s}}\exp(-d_1 s) + 2\sqrt{d_1} - 2\sqrt{d_1}\,\mathrm{erfc}\left(\sqrt{d_1 s}\right) ds,$$

$$\tau_2(t) = \frac{\exp(-d_1 t)}{\sqrt{\pi t}} + \sqrt{d_1} - \sqrt{d_1}\,\mathrm{erfc}\left(\sqrt{d_1 t}\right),$$

$$\tau_3(t) = \frac{Gr_1\exp(-d_1 t)}{\sqrt{\pi t}} + Gr_1\sqrt{d_1} - Gr_1\sqrt{d_1}\,\mathrm{erfc}\left(\sqrt{d_1 t}\right),$$

$$\tau_4(t) = \frac{Gr_1\exp(-d_1 t)}{\sqrt{\pi t}} + Gr_1\exp(d_3 t)\sqrt{d_1 + d_3} -$$

$$Gr_1\exp(d_3 t)\sqrt{d_1 + d_3}\,\mathrm{erfc}\left(\sqrt{d_1 t + d_3 t}\right),$$

$$\tau_5(t) = \frac{Gr_1\sqrt{\mathrm{Pr}_1}}{\sqrt{\pi t}},$$

$$\tau_6(t) = \frac{Gr_1\sqrt{\mathrm{Pr}_1}}{\sqrt{\pi t}} + Gr_1\exp(d_3 t)\sqrt{\mathrm{Pr}_1 d_3} - Gr_1\exp(d_3 t)\sqrt{\mathrm{Pr}_1 d_3}\,\mathrm{erfc}\left(\sqrt{d_3 t}\right).$$

Nusselt number *Nu* is defined as

$$Nu = -\left[\frac{\partial T}{\partial z}\right]_{z=0} = \frac{\sqrt{\mathrm{Pr}_1}}{\sqrt{\pi t(Rd + 1)}}. \tag{22}$$

RESULTS AND DISCUSSION

Further analysis on the MHD non-coaxial rotation flow and heat transfer characteristics for an accelerated disk along with the radiation effect is conducted with the assistance of pictorial discussion. Due to the rotating system, there exist a Coriolis force which can deflect the fluid flow and lead to the formation of a secondary flow. The present study can be practically applied in the engineering field such as in food processing industries (mixer machines and stirrers with two kneaders) and electronic devices (cooler pad with two fan). The velocity (primary and secondary) and temperature distributions are graphically plotted under the influences of different values of radiation parameter *Rd*, acceleration parameter *A*, porosity parameter *K*, Grashof number *Gr*, magnetic parameter *M*, and Prandtl number Pr by using MathCAD software. Due to the existence of primary and secondary velocities in Equation (17), the numerical coding in MathCAD is separated by two parts: the real and imaginary parts. The values of parameter are selected by referring to Mohamad et al. (2020). The investigation of their behavior is conducted by assigning the parameters to the values of $Rd = 2$, $K = 2$, $M = 2$, $Gr = 5$, $\mathrm{Pr} = 6.2$. The pictorial illustrations of their effects are presented in Figures 2 to 10. In this study, the effects of *Gr*, *K*, and *M* can be addressed in the primary and secondary velocity profiles only because these parameters exist in the momentum equation. However, the presence of *Rd* in all the governing equations has caused all profiles are under its influences. Meanwhile, Table 1 and Figures 11-14 show the results of skin friction τ and Nusselt number *Nu*. As the verification for present solution, the results published by Guria et al. (2009) was used as the benchmark for this solution by allowing parameters of magnetic *M*, suction *S* and slip condition equal to zero. Taking $M = Rd = A = Gr = 0$ and $K \to \infty$ in the present result, the comparison is found to be in excellent agreement as shown in Figure 2. Hence, the obtained solution is valid.

When the flow is close to the surface, the primary velocity *f* is larger, and it gradually decreases as the fluid flows away from the surface. Meanwhile, the secondary velocity *g* grows until it reaches the highest velocity in the range of $0 \le z \le 1$ and then declines when the flow is distant from the surface. Due to the enforced wall temperature, the highest temperature is obtained when the fluid is near the surface, and it then declines as the fluid moves away from the surface.

The physical characteristics of the velocity (primary and secondary) and temperature propagation under the effect of *Rd* are exhibited in Figures 3 and 4. Figure 3 indicates that the rising value of *Rd* results in the increase of both velocity profiles. As the intensity of the radiation increases, the fluid absorbs a huge amount of heat which directly contribute in the enlargement of thermal boundary layer and an augment of the temperature profile as in Figure 4. The heated fluid then causes bonds between the fluid particles to weaken and thus, the fluid's viscosity reduces. Hence, it leads to the

elevation of both primary and secondary velocities. The momentum boundary layer had augmented in response with the increase of *Rd*.

Meanwhile, the impact of implementing an accelerated disk *A* in the fluid flow are shown in Figure 5. As the level of disk acceleration A increases, the external force from disk movement will supply more energy for the fluid to flow faster. Likewise, the porosity K has given the same effects on the behavior of primary and secondary flow as illustrated in Figure 6. A clear impact of *K* can be observed with the assistance of zooming box. Increasing values of *K* have boosted the thrust force of the fluid due to a decrease in frictional force within the medium. In other words, the fluid can effortlessly flow within high porosity medium and causing an increase in both velocity profiles (primary and secondary). Next, the identical changes of *K* on velocity (primary and secondary) profiles are also observed under the impact of *Gr* which is displayed in Figure 7. In the physical sense, *Gr* is the ratio of buoyancy force to viscous force. Increasing values of *Gr* imply to the stronger of buoyancy force which eventually diminishes the viscous force and results in an accelerated primary and secondary velocity profiles.

However, a reverse effect is noticed in Figures 8 and 9. When the values of *M* and Pr ascend, the primary and secondary velocities decline. This is because the higher values of *M* in Figure 8 indirectly increase the drag force acting on the fluid which is known as the Lorentz force. Thus, reducing velocity of the fluid as the fluid is flowing with high resistance. Then, Figure 9 shows that increasing the value of Pr causes the primary and secondary velocities to decrease. This is because the fluid's viscosity increases and reduces thermal diffusivity which results in a decline in fluid flow. Apart from that, the same change is found in temperature profile in Figure 10 as a fall in temperature profile is observed when Pr increases. The physical verification to this deterioration is that high Pr value has poorer thermal conductivity, which decreases the amount of heat transfer and as a result, temperature reduces.

The skin friction τ and Nusselt number *Nu* for embedded parameters are evaluated and presented in Table 1 and Figures 11-14, respectively. It is found that τ decreases when the values of parameters *Rd*, *K* and *Gr* increase while a reverse effect on τ is recorded for increasing values of parameter *M* and Pr. The decrease of τ in response to *Rd*, *K*, and *Gr* indicates that the fluid under these particular effects has a low shear stress at the wall which is a factor of increasing velocity. From Figure 14, it is obvious that the effect of increasing values of *Rd* and Pr on *Nu* is quite opposite to the effects on temperature and also opposite to each other. From these results, it suggested that a heating process and phenomenon can be sustained by controlling the level of *Rd* since its increasing can reduce the rate of heat transfer.

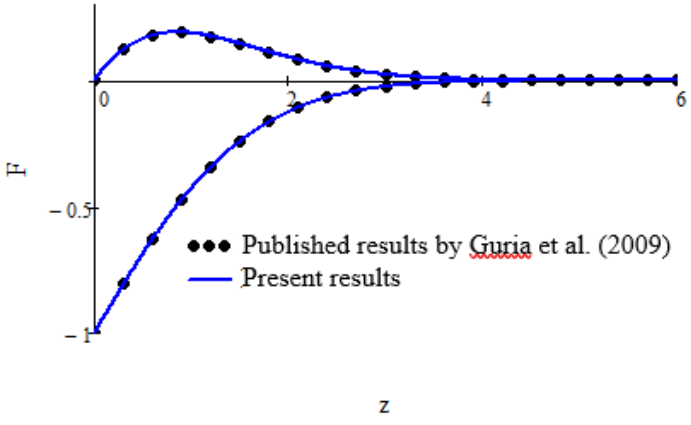

FIGURE 2. Verification of present results with published results by Guria et al. (2009)

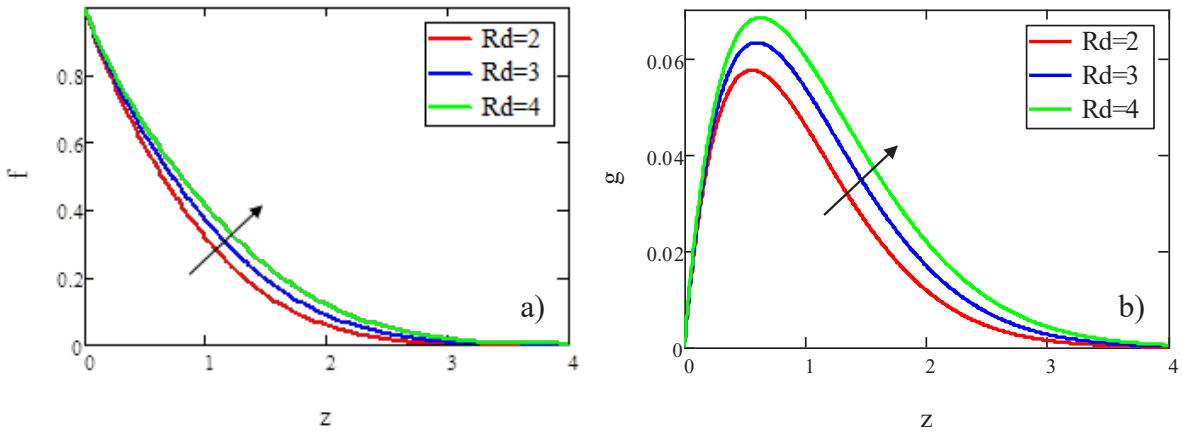

FIGURE 3. f (a) and g (b) profiles for several values of Rd

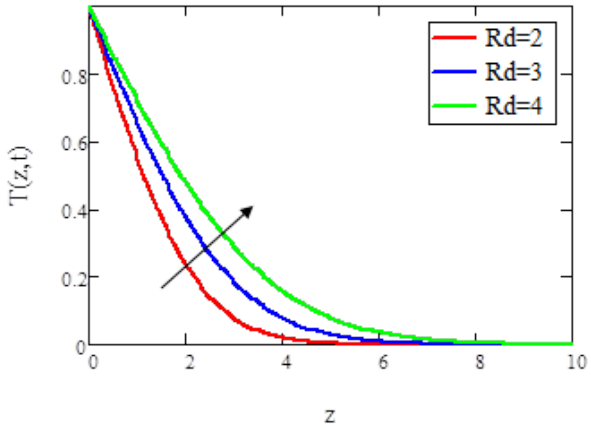

FIGURE 4. T(z,t) profile for several values of Rd

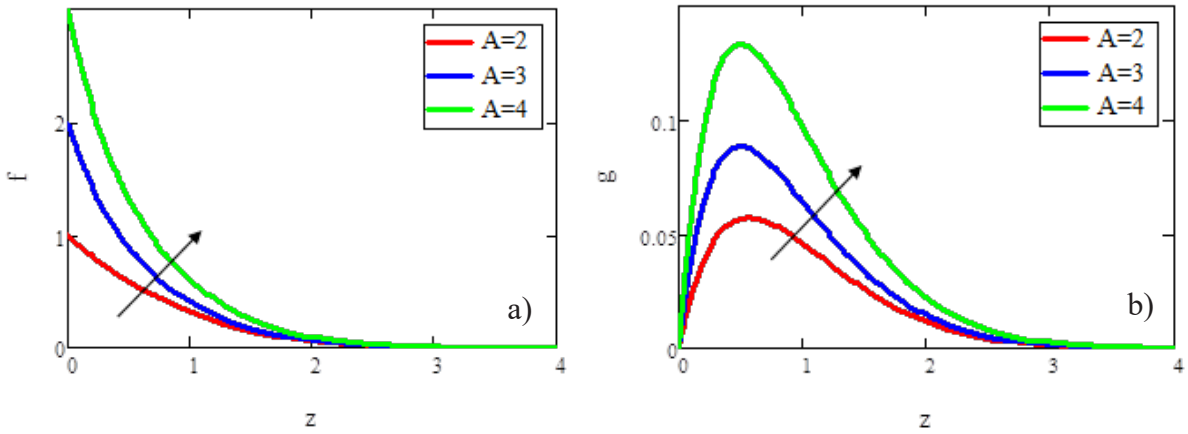

FIGURE 5. f (a) and g (b) profiles for several values of A

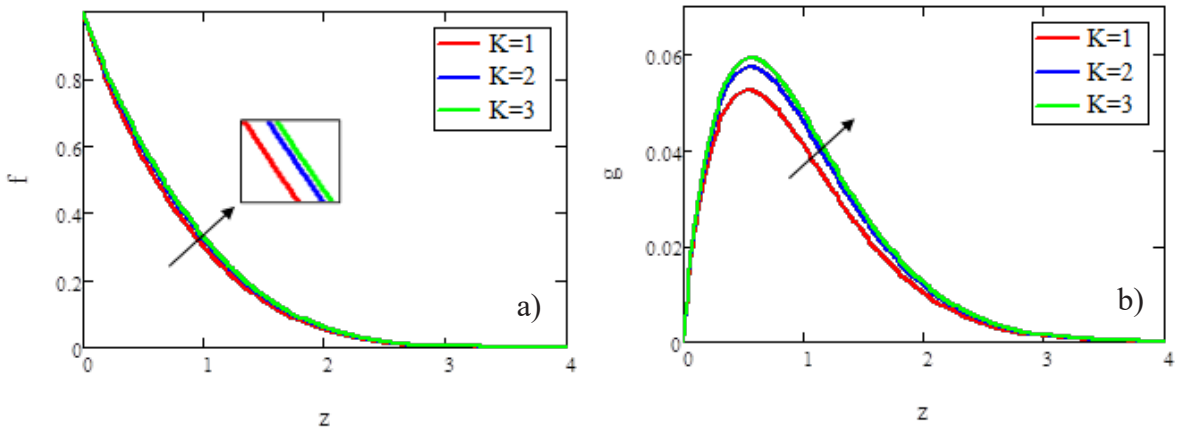

FIGURE 6. f (a) and g (b) profiles for several values of K

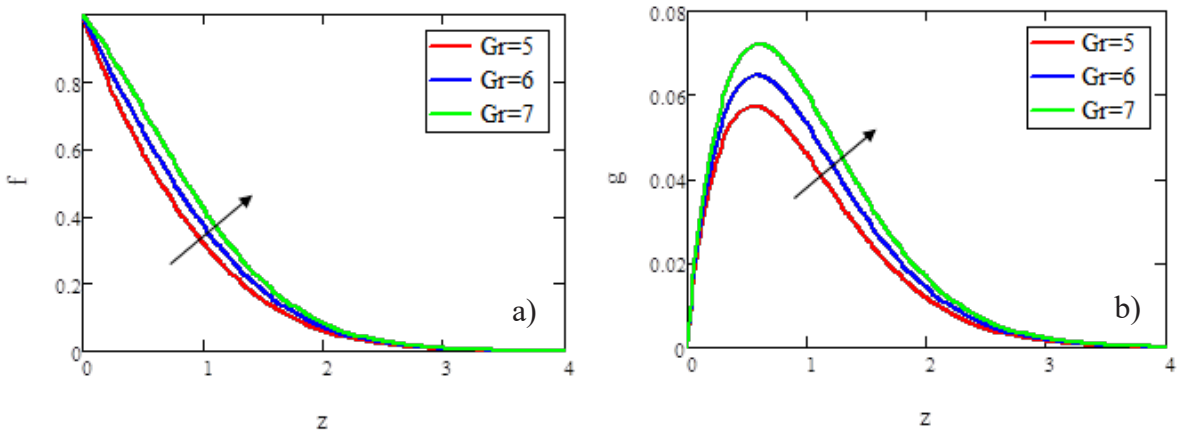

FIGURE 7. f (a) and g (b) profiles for several values of Gr

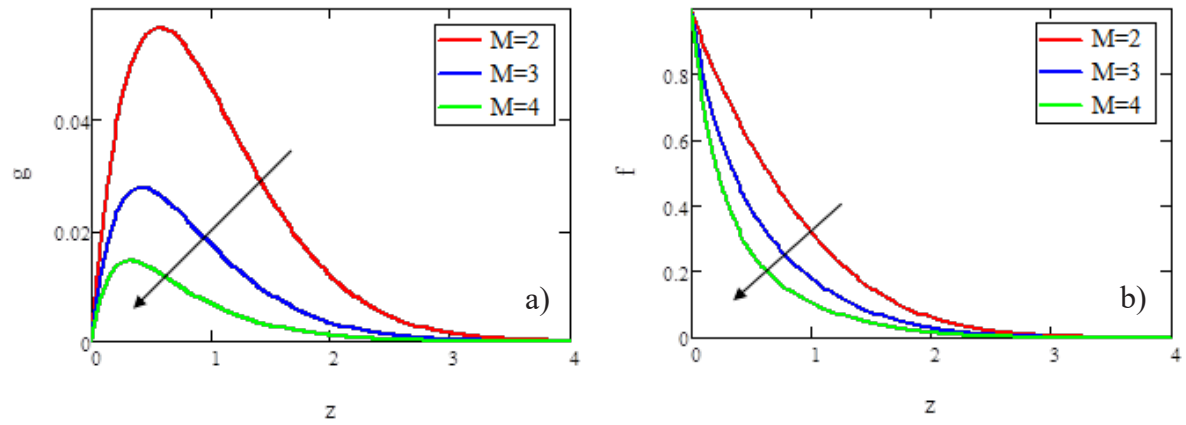

FIGURE 8. f (a) and g (a) profiles for several values of M

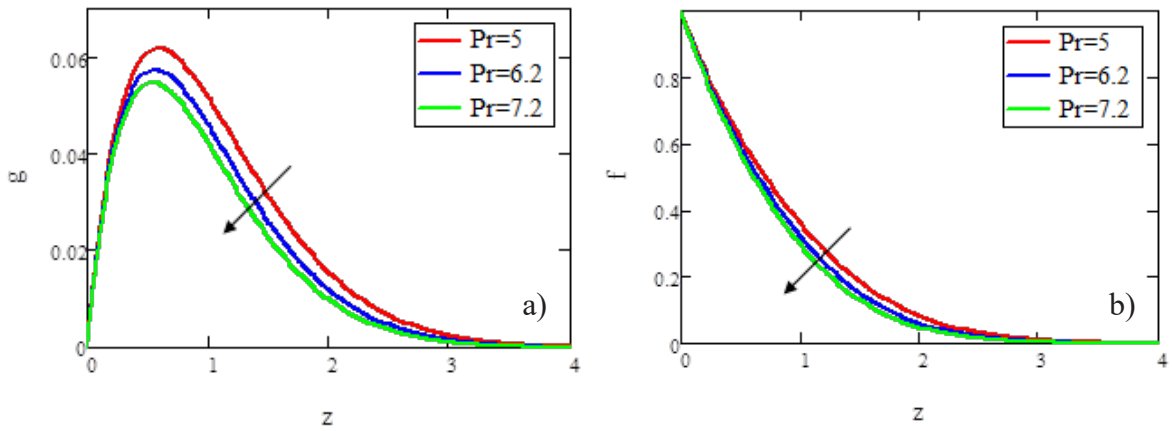

FIGURE 9. f (a) and g (a) profile for several values of Pr

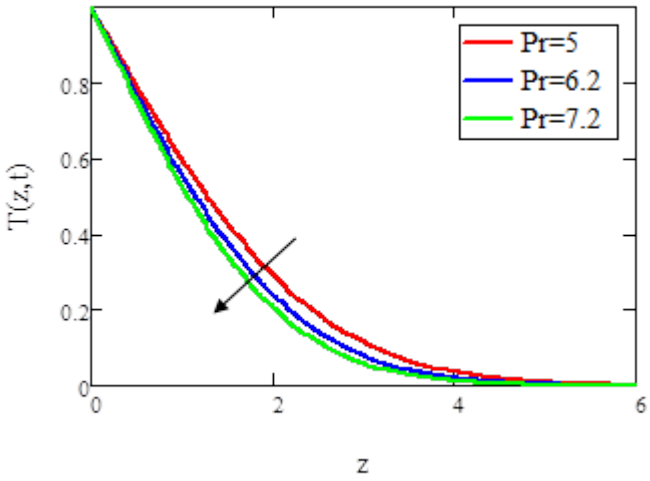

FIGURE 10. $T(z, t)$ profile for several values of Pr

TABLE 1. Skin friction

Rd	Pr	τ	
		Primary	Secondary
2	**6.2**	1.068	-0.278
3	6.2	0.990	-0.289
4	6.2	0.932	-0.298
2	**7.2**	1.110	-0.272
2	**9.0**	1.175	-0.264

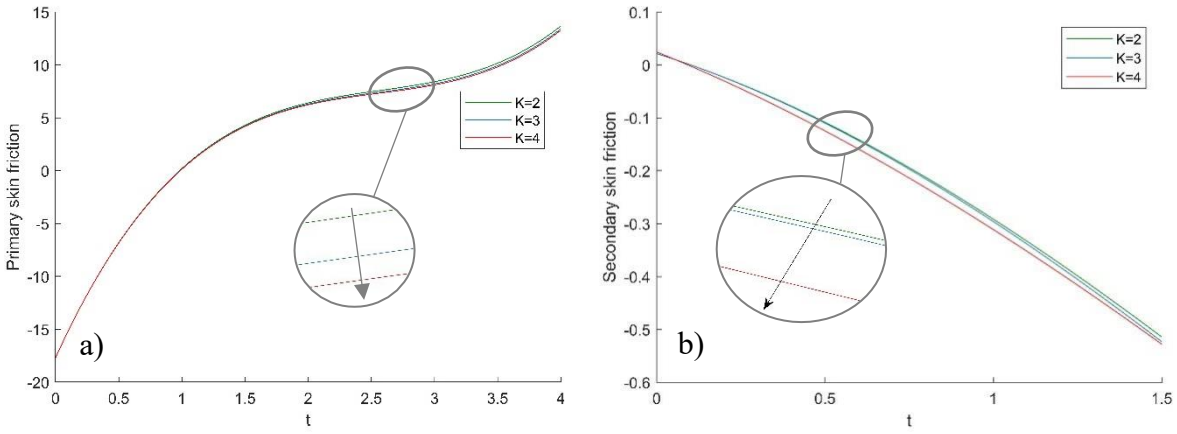

FIGURE 11. Variation of primary (a) and secondary (b) skin friction for different values of *K*

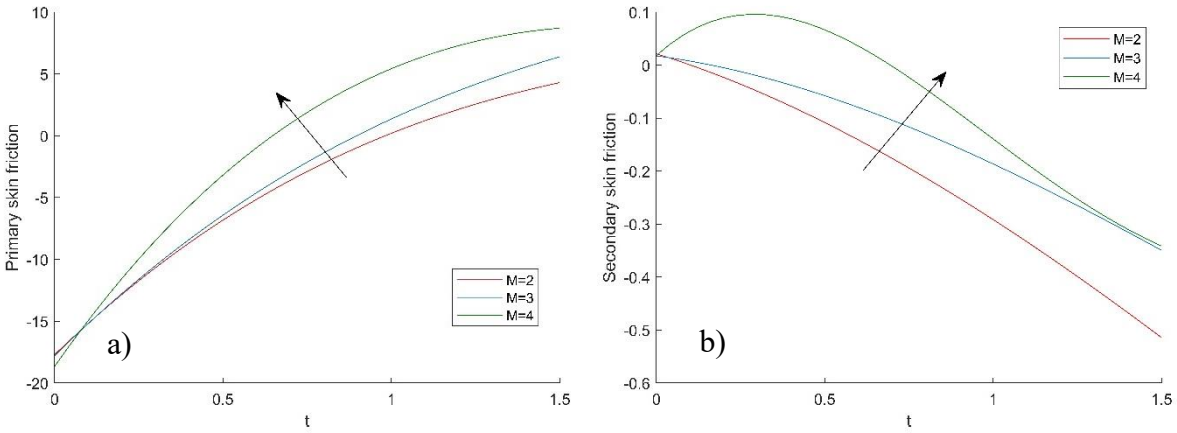

FIGURE 12. Variation of primary (a) and secondary (b) skin friction for different values of *M*

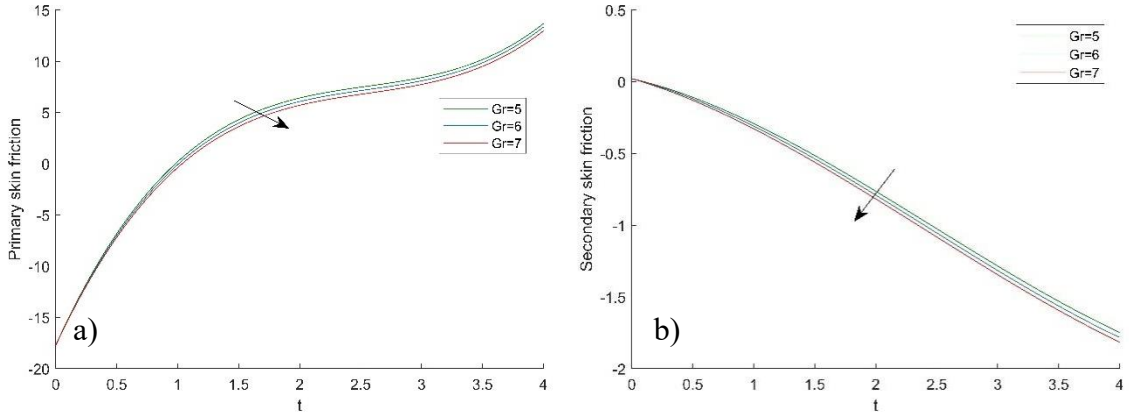

FIGURE 13. Variation of primary (a) and secondary (b) skin friction for different values of *Gr*

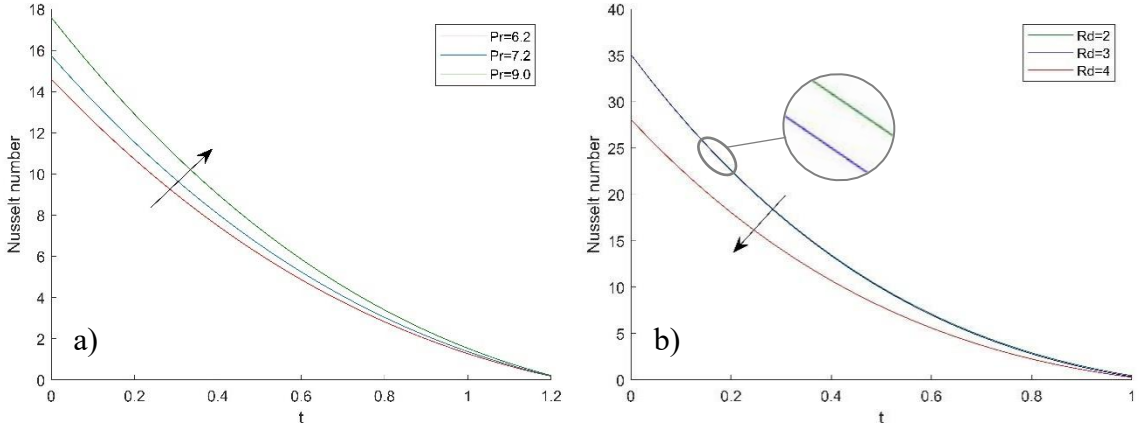

FIGURE 14. Variation of Nusselt Number for different values of Pr (a) and *Rd* (b)

CONCLUSION

The unsteady mixed convection flow of viscous fluid under the influence of non-coaxial rotation has attracted much attention around the world research. So, this study focuses on an accelerating vertical disk and includes the effects of thermal radiation, magnetic field and porosity as well. The problem is tackled by using the Laplace transform technique and the solutions are graphically plotted using MathCAD. The velocity profiles are enhanced with an increase of *A*, *Rd*, *K*, and *Gr*. While, Pr and *M* cause a deterioration in the velocity profiles. A growth in temperature distribution is observed for increasing *Rd*. While, this parameter has an opposite effect on the rate of heat transfer. The impact of intensifying *Rd* can be beneficial to the improvement of heating instruments as its reduction in heat transfer rate implies to the decreasing of heat loss and it is important to sustain a certain temperature environment. The exact solution obtained from this problem can be the benchmark for verification of other numerical and approximate solutions. This study can be a good reference for researchers and educators, as well as build a better understanding on the real fluid mechanic problems.

ACKNOWLEDGEMENTS

The authors would like to acknowledge the Ministry of Higher Education, Malaysia and Research Management Centre-UTM, Universiti Teknologi Malaysia (UTM) for financial supports through vote numbers FRGS/1/2019/STG06/UTM/02/22, 17J98, 4B583, 02M40 and 08G33. The authors declare that they have no conflicts of interest to report regarding the present study.

REFERENCES

Amin, W.N.Z., Mohamad, A.Q., Shafie, S. & Qasim, M. 2020. G-Jitter fully developed heat and mass transfer by mixed convection flow between two parallel plates with constant heat flux. *Sains Malaysiana* 49(5): 1201-1208.

Asghar, S., Hanif, K., Hayat, T. & Khalique, C.M. 2007. MHD non-Newtonian flow due to non-coaxial rotations of an accelerated disk and a fluid at infinity. *Communications in Nonlinear Science and Numerical Simulation* 12(4): 465-485.

Bakar, N.A., Roslan, R., Karimipour, A. & Hashim, I. 2019. Mixed convection in lid-driven cavity with inclined magnetic field. *Sains Malaysiana* 48(2): 451-471.

Berker, R. 1963. *Handbook of Fluid Dynamics.* Berlin: Springer.

Das, S. & Jana, R.N. 2014. Hall effects on unsteady hydromagnetic flow induced by an eccentric-concentric rotation of a disk and a fluid at infinity. *Ain Shams Engineering Journal* 5(4): 1325-1335.

Das, S., Maji, S.L., Ghara, N. & Jana R.N. 2012. Combined effects of Hall currents and slip condition on steady flow of a viscous fluid due to non-coaxial rotation of a porous disk and a fluid at infinity. *Journal of Mechanical Engineering Research* 4(5): 175-184.

Erdogan, M.E. 2000. Flow induced by non-coaxial rotation of a disk executing non-torsional oscillations and a fluid rotating at infinity. *International Journal of Engineering Science* 38(2): 175-196.

Ersoy, H.V. 2017. Unsteady flow due to a disk executing non-torsional oscillation and a Newtonian fluid at infinity rotating about non-coaxial axes. *Sādhanā* 42(3): 307-315.

Guria, M. 2018. Unsteady MHD flow due to non-coaxial rotations of a porous disk and a fluid at infinity subjected to a periodic suction. *International Journal of Applied Mechanics and Engineering* 23(3): 623-633.

Guria, M., Das, S. & Jana, R.N. 2007. Hall effects on unsteady flow of a viscous fluid due to non-coaxial rotation of a porous disk and a fluid at infinity. *International Journal of Non-Linear Mechanics* 42(10): 1204-1209.

Guria, M., Kanch, A.K., Das, S. & Jana, R.N. 2009. Effects of Hall current and slip condition on unsteady flow of a viscous fluid due to non-coaxial rotation of a porous disk and a fluid at infinity. *Meccanica* 45(1): 23-32.

Hayat, T., Ellahi, R. & Asghar, S. 2008. Hall effects on unsteady flow due to non-coaxially rotating disk and a fluid at infinity. *Chemical Engineering Communications* 195(8): 958-976.

Hussain, S.M., Johsi, H.J. & Seth, G.S. 2018. Radiation effect on MHD convective flow of nanofluids over an exponentially accelerated moving ramped temperature plate. In *Applications of Fluid Dynamics,* edited by Singh, M., Kushvah, B., Seth, G. & Prakash, J. Lecture Notes in Mechanical Engineering. Singapore: Springer. pp. 31-43. https://doi.org/10.1007/978-981-10-5329-0_3

Ishak, A. 2011. MHD boundary layer flow due to an exponentially stretching sheet with radiation effect. *Sains Malaysiana* 40(4): 391-395.

Mahanthesh, B., Brizlyn, T., Shehzad, S.A. & Gireesha, B.J. 2019. Nonlinear thermo-solutal convective flow of Casson fluid over an oscillating plate due to non-coaxial rotation with quadratic density fluctuation. *Multidiscipline Modeling in Materials and Structures* 15(4): 818-842.

Maji, L., Manna, G., Guria, M. & Jana, R.N. 2010. Unsteady flow due to non-coaxial rotation of a porous disk and a fluid at infinity through porous medium. *Chemical Engineering Communications* 197(6): 791-803.

Mohamad, A.Q., Ismail, Z., Omar, N.F.M., Qasim, M., Zakaria, M.N., Shafie, S., Jiann, L.Y. 2020. Exact solutions on mixed convection flow of accelerated non-coaxial rotation of MHD viscous fluid with porosity effect. *Defect and Diffusion Forum* 399: 26-37.

Mohamad, A.Q., Khan, I., Ismail, Z. & Shafie, S. 2016. Exact solutions for unsteady free convection flow over an oscillating plate due to non-coaxial rotation. *Springerplus* 5(1): 2090.

Mohamad, A.Q., Khan, I., Jiann, L.Y., Shafie, S., Isa, Z.M. & Ismail, Z. 2018. Double convection of unsteady MHD non-coaxial rotation viscous fluid in a porous medium. *Bulletin of the Malaysian Mathematical Sciences Society* 41(4): 2117-2139.

Mohamad, A.Q., Khan, I., Zin, N.A.M., Isa, Z.M., Shafie, S. & Ismail, Z. 2017. Mixed convection flow on MHD non-coaxial rotation of second grade fluid in a porous medium. *AIP Conference Proceedings* 1830(1): 020044.

Noranuar, W.N.N., Mohamad, A.Q., Shafie, S. & Khan, I. 2021. Accelerated non-coaxial rotating flow of MHD viscous fluid with heat and mass transfer. *IOP Conference Series: Materials Science and Engineering* 1051(1): 012044.

Noranuar, W.N.N., Mohamad, A.Q., Shafie, S., Khan, I. & Jiann, L.Y. 2020. Radiative non-coaxial rotation of magnetohydrodynamic Newtonian carbon nanofluid flow in porous medium with heat and mass transfer effects. *Journal of Nanofluids* 9(4): 321-335.

Pandit, K.K., Singh, S.I. & Sarma, D. 2018. Heat and mass transfer analysis of an unsteady MHD flow past an impulsively started vertical plate in presence of thermal radiation. *International Journal of Fluid Mechanics & Thermal Sciences* 4(2): 18-26.

Rafiq, S., Nawaz, M. & Mustahsan, M. 2018. Casson fluid flow due to non-coaxial rotation of a porous disk and the fluid at infinity through a porous medium. *Journal of Applied Mechanics and Technical Physics* 59(4): 601-607.

Rana, S., Iqbal, M.Z., Nawaz, M., Khan, H.Z.I., Alebraheem, J. & Elmoasry, A. 2020. Influence of chemical reaction on heat and mass transfer in MHD radiative flow due to non-coaxial rotations of disk and fluid at infinity. *Theoretical Foundations of Chemical Engineering* 54(4): 664-674.

Seth, G.S., Sarkar, S. & Hussain, S.M. 2014. Effects of Hall current, radiation and rotation on natural convection heat and mass transfer flow past a moving vertical plate. *Ain Shams Engineering Journal* 5(2): 489-503.

Srivastava, N. 2017. MHD flow between two non-coaxial disks rotating at different speeds. *Rendiconti del Circolo Matematico di Palermo* 67: 173-184.

Zainuddin, N., Hashim, I., Saleh, H. & Roslan, R. 2016. Effects of radiation on free convection from a heated horizontal circular cylinder in the presence of heat generation. *Sains Malaysiana* 45(2): 315-321.

*Corresponding author; email: ahmadqushairi@utm.my